ARTICLE

Variations in crystals of flufenamic acid of its methyl and *tert*-butyl analogues as impurities as determined by partial dissolutions

Received 00th January 20xx,
Accepted 00th January 20xx

DOI: 10.1039/x0xx00000x

Timothy Bourke[a], Renato A. Chiarella[b] and Humphrey A. Moynihan*[a]

Achieving specified levels of impurities is one the key goals of crystallisation processes in manufacturing. The mode of impurity incorporation and the variation of impurity levels throughout crystal batches are key factors affecting the performance of crystallisations in terms of achieving purity specifications. Evaluation of the distribution of impurities in crystals of flufenamic acid (FFA) using a controlled partial dissolution approach is described. 2-(3-Tolylamino)benzoic acid (MeFA) and 2-((3-(*tert*-butyl)phenyl)amino)benzoic acid (*t*BuFA*)*, analogues of FFA in which the trifluoromethyl group has been replaced by a methyl group or by a *tert*-butyl group respectively, were selected as the impurities. Thermal analysis suggests formation of a solid solution between FFA and MeFA isostructural to FFA Form III. The stepwise dissolution approach was initially demonstrated on samples of pure FFA crystals and was then extended to evaluate the distribution of levels of MeFA and *t*BuFA impurities. The impurity levels are shown as varying with dissolution midpoint. Stepwise dissolution was usefully applied to FFA crystal of various morphologies, while for crystals with extremely needle-like morphology, a segmentation analysis approach was more practical. The work presented outlines a method for evaluating the distribution of impurities in crystalline materials using commonly available analytical and particle sizing methods.

Introduction

Crystallisation is a major method of product isolation and purification in pharmaceutical and fine chemical manufacturing.[1] As such, crystallisation plays a key role in the management of impurities in the manufacturing process and the behaviour of process impurities during the crystallisation process is a key determinant in the outcome. Achieving acceptable purity can be especially challenging when crystals are retained in the solid product.[2] In such cases, the mode of inclusion of the impurities in the solid product is a significant issue as well as the uniformity, or otherwise, of the levels of impurities throughout the solid product.[3] Elucidating the mode of inclusion of impurities can be a significant challenge[4,5,6] but can facilitate process design and optimisation.[7]

Typically, the level of a particular impurity present in a batch of crystallised material is measured, often by HPLC, as an overall level for the batch. Such a measurement does not seek to evaluate any variation in the impurity level within a batch, which may vary in a number of ways. For example, it is possible that there may be some variation between crystal particles. It is also possible that there may be variations within individual crystal particles relating to differing levels of incorporation during the stages of crystal growth.[1] Impurities may also be present in greater quantities on the surfaces of crystal particles due to inadequate washing[8,9] and other variations of impurity level may be possible. Evaluation of such variations in impurity levels requires sampling and analytical methods which provide impurity level data which can be assigned to definable locations within a crystal batch. Analytical technologies such as secondary ion time-of-flight mass spectrometry and fluorescence staining have been shown to be suitable.[10,11,12] Recognising that HPLC is a very widely used analytical method in pharmaceutical process development, and noting that analysis by HPLC requires sample dissolution, we have sought to develop approaches which utilise selective dissolution methods to provide impurity level data which can be assigned to definable spatial locations in crystal batches.[13,14] These methods were developed using simple model systems while the present work seeks to apply these approaches to a significant pharmaceutical system, for which the non-steroidal anti-inflammatory compound flufenamic acid[15] was selected. Flufenamic acid (FFA) displays many of the material issues typical of modern APIs such as polymorphism.[16,17] The work described herein aims to map the level of specific impurities within FFA batches and also develops approaches which are suitable for particles with difficult morphologies such as fine needles.

Previous work utilised isosteres of the trifluoromethyl group in the selection of impurities with good tendency for incorporation into growing crystals.[13,18] As FFA contains a trifluoromethyl group, an isostere such as the methyl analogue

[a] *Analytical and Biological Chemistry Research Facility / School of Chemistry / Synthesis and Solid State Pharmaceutical Centre, University College Cork, College Road, Cork Y12 K8AF, Ireland.*
[b] *Pharmaceutical Development, Alkermes Inc., 900 Winter Street, Waltham, MA 02451, USA.*

Electronic Supplementary Information (ESI) available: Synthesis details; IR, ^{1}H NMR and ^{13}C NMR spectra; HPLC calibration data, PXRDs, solubility data, morphology images, DSCs. See DOI: 10.1039/x0xx00000x

MeFA (Scheme 1) is a good candidate for an impurity which is likely to be well retained in FFA crystals. To provide contrasting, less predictable behaviour, the FFA analogue in which the trifluoromethyl groups was replaced by the sterically demanding *tert*-butyl group (*t*BuFA, Scheme 1) was also selected.

Experimental

Flufenamic acid and analogues

Flufenamic acid was purchased from Merck. A modification of a literature[19] route to fenamic acids was used to obtain analogues of FFA in which the trifluoromethyl group was replaced by a methyl group (MeFA) or by a *tert*-butyl group (*t*BuFA) (Scheme 1). Full details of the syntheses are given in the in the ESI.

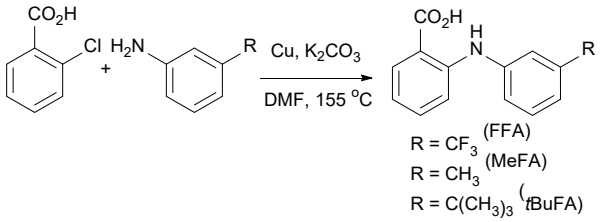

Scheme 1 Preparation and structures of FFA and the MeFA and tBuFA analogues.

Analytical methods

HPLC. HPLC data was obtained from an Agilent 1290 Infinity II LC System interfaced to a Dell OptiPlex 5040. A reversed-phase UHPLC C18 column (Zorbax Eclipse Plus, 2.1 x 50 mm, 1.8 µm particle size) was used, with a mobile phase consisting of 50:50 ratio of acetonitrile and a 0.1% v/v aqueous solution of trifluoroacetic acid, flow rate of 0.5 mL min^{-1}, injection volume of 2 µL, and column temperature of 30 °C. The detector was set at 280 nm. Instrument control and data processing was performed using Agilent OpenLab ChemStation software. Information on calibration curves and regression analysis is provided in the ESI.

PXRD. PXRD was performed at ambient temperature using a Stoe Stadi MP diffractometer operating in transmission mode with a linear PSD detector with an anode current of 40 mA, an accelerating voltage of 40 kV and Cu $K\alpha_1$ radiation (λ = 1.5406 Å) scanning in steps of 1.0° for 30 seconds per step from 5° to 35° in 2θ. Samples were held between acetate foils.

DSC. DSC analysis was carried out on a TA Q1000 Calorimeter with an RCS 40 cooling system. Ramping was carried out from approximately 15 °C to 180 °C in aluminium pans at a heating rate appropriate to the experiment. Mass of samples were between 2 mg to 5 mg.

Materials

FFA Polymorphs. FFA is highly polymorphic and there is extensive literature on the preparation and stability of different FFA polymorphs.[16, 20-23] The commercially available material is Form I (ESI Figure S19). Form III is known to be the most thermodynamically stable form at typical room temperatures (18 °C – 25 °C) and Form III was selected as the primary polymorph for this work. FFA material was recrystallised from methanol or acetonitrile before use and confirmed as Form III (ESI Figure S20).

Crystallisation of FFA material. Crystals of FFA were grown from acetonitrile or methanol solutions. For growth from acetonitrile, material was suspended in a volume of acetonitrile giving a solution of ca. 1.5 times the saturation point (utilising the solubility data given in the ESI Fig. S21), heated in an oil bath to 80 °C to complete dissolution and allowed to cool over 3 hours. The crystals were washed with cold hexane and fully dried *via* a high-vacuum line. For crystallisation from methanol, the required amount of material was dissolved to give a subsaturated solution which was filtered through a syringe filter and allowed to evaporate until crystals had formed and the crystals washed with cold hexane and dried over vacuum.

FFA crystals, whether pure or containing MeFA or *t*BuFA impurities, generally had an elongated morphology. Growth from methanol could be used to provide relatively prismatic crystals while crystals grown from acetonitrile were more acicular. Both were similar to literature morphologies for FFA Form III.[24,25] The presence of the MeFA or *t*BuFA impurities tended to result is somewhat smaller or thinner crystals, again consistent with literature observations.[20,25] FFA crystals with more acicular or less prismatic morphologies were often obtained and partial dissolution methods could also be applied to such crystals. However, some crystals grew as extremely long fine needles from a common nucleation point and a segmentation analysis method was used for these crystals, as described below. Images of the various crystal morphologies obtained are shown in the ESI Figs S22 to S24. In the results given below, the proportion of MeFA or *t*BuFA impurity is given as a percentage of the total number of moles.

Partial dissolutions. The sample crystals were suspended in a glass vial in a volume of hexane sufficient to dissolve approximately 10% of the sample mass, based on the solubility of the material in hexane (2.40 mg ml^{-1} at 25 °C). The suspension was agitated at a rate of 300-500 rpm for 90 minutes using Fisherbrand ZX3 Vortexer or a VWR Incubating Orbital Mini Shaker.

Crystal sizing. Images of the individual crystal particles were captured using a Nikon Eclipse 50i polarising microscope with a Nikon Digital Sight DS-Fi1 digital camera. NIS-Elements software version BR 3.1 was used to analyse the images. An Honor 7x dual 16 MP camera with High Dynamic Range and Phase Detection Auto Focus was used to capture digital macro photographs of the larger prismatic crystals, using ImageJ image analysis software.[26,27] Mass values were measured before and after a dissolution stage using a Mettler Toledo MT5 microbalance (±0.0008 mg).

Segmentation analysis. Intact crystals were arranged on glass slides and oriented in the direction of growth. Each crystal was divided lengthwise into three segments of approximately equal length.

Results and discussion

The aim of this work was to apply a controlled partial dissolution approach to evaluating the distribution of impurities in crystals of flufenamic acid (FFA). FFA analogues in which the trifluoromethyl group was replaced by a methyl group (i.e.,

MeFA) or a *tert*-butyl group (i.e., *t*BuFA) were selected to give the impurities for study. MeFA was selected to be an impurity likely to be well incorporated into FFA crystals, as the CF_3 and CH_3 groups are relatively isosteric, for example, their respective van der Waals radii are 2.15 Å and 2.0 Å,[18] while *t*BuFA was selected to be less predictably well incorporated, owing to the greater steric demand of the *tert*-butyl group. A modification of a literature[19] route to fenamic acids was used to obtain the MeFA and *t*BuFA analogues (Scheme 1).

The polymorphism of FFA[16, 20-23] is a complicating factor in examining the impact on FFA phase behaviour on the presence of an impurity in the solid material, especially a structurally similar impurity. The case of mefenamic acid as an inclusion in FFA material was studied in detail by Lee and Byrn and formation of a FFA Form III / mefenamic acid solid solution was proposed.[20] MeFA, having replacement of the CF_3 group of FFA by a CH_3 group as the only point of difference, could be regarded as an even closer structural analogue to FFA than mefenamic acid. In our work, the DSC behaviour of pure FFA was found to display melting of Form III, followed by recrystallisation and melting of Form I (ESI Figure S25). Lower heating rates and sample grinding were found to reduce observation of the Form III melting endotherm and increase observation of the Form I endotherm, while higher heating rates and leaving samples unground had the opposite effect. DSC of FFA crystals containing quantities of MeFA displayed the same thermal events with changes to the extent of the Form III and Form I melting endotherms (ESI Fig. S26), in line with those reported by Lee and Byrn.[20]

Given the close structural similarity between FFA and MeFA and comparison with the thermal behaviour of the FFA Form III / mefenamic acid system, solid solution formation is also likely in the FFA III / MeFA case. This is also supported by the gradual transformation of PXRD pattern from that of pure FFA Form III to that of pure MeFA with increasing proportion of MeFA (ESI Fig. S27). To follow the effect on the melting behaviour of FFA Form III of increasing MeFA content, a series of DSC scans were carried out at a heating rate of 20 °C min^{-1} to enhance observation of the Form III melting endotherm as noted above. Multiple repeated scans were carried out at each MeFA mole fraction, with the results summarised in Figure 1. Depression of FFA Form III melting point with increasing MeFA level was observed up to MeFA levels of ca. 40%. At ca. 50% MeFA, the melting point depression plateaus while at higher MeFA levels, melting point increases, which can also be interpreted as decrease in melting point of pure MeFA with increasing FFA level. The data is consistent with formation of a solid solution with a minimum melting point, or thermal minimum, for the FFA Form III / MeFA system. DSC analysis of FFA materials containing between 2 to 5 % *t*BuFA was carried out (ESI Figure S28). *t*BuFA appears to have a similar effect as MeFA on suppressing the polymorphic transition of FFA, favouring the appearance of the Form III melting endotherm and reducing that of Form I with increasing *t*BuFA inclusion.

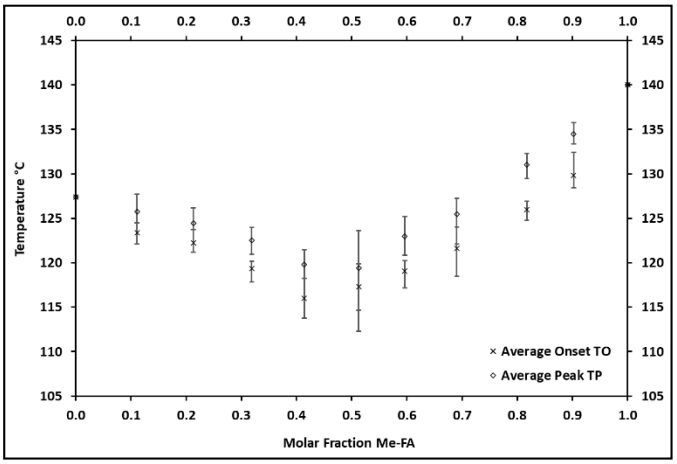

Fig. 1 Ranges of onset (T_O) and peak (T_P) temperatures of the FFA Form III melting endotherm measured from DSC curves of crystalline FFA containing increasing levels of MeFA. DSC scans were recorded at 20 °C min^{-1}, with multiple repetitions for each MeFA mole fraction. The average temperature and range of temperatures for the T_O and T_P values for each MeFA mole fraction are shown.

Figure 2 shows a view of the unit cell of FFA Form III.[28] The molecules are orientated in the unit cell in such a way that the trifluoromethyl groups of two molecules are facing each other, at a distance of 4.156 Å (C···C) or 3.038 Å (F···F). A molecule of MeFA, in which the CF_3 group is simply replaced by a CH_3 group, would be accommodatable within the FFA Form III structure and a degree of C-H···F hydrogen bonding might be possible. These features and the observation of solid solution formation for the FFA Form III / MeFA system are compatible.

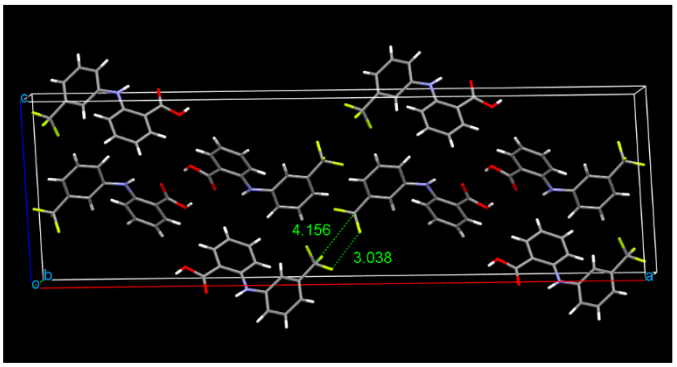

Fig. 2 View of the unit cell of FFA Form III FFA[28], showing the orientation of the -CF_3 groups relative to each other and the distance between the groups.

For analysis of the distribution of the MeFA and *t*BuFA impurities, crystals of FFA containing 2% to 5% levels of MeFA or *t*BuFA were grown by slow evaporation from methanol solutions. The size and morphology of crystals containing MeFA impurity were similar to those of pure FFA while crystals containing *t*BuFA were smaller. The correlation between MeFA levels in solution and incorporation into FFA crystals grown from methanol is shown in Figure 3. The incorporation could also be quantified as a ratio of impurity levels in the crystal samples to levels of the impurity in solution from which the crystals were grown, which gave a ratio of 1.06 ± 0.03 for MeFA

in FFA crystals grown from MeOH. Crystals of FFA grown from MeOH containing levels of *t*BuFA impurity exhibited an average incorporation ratio of 1.24 ± 0.12. Both impurities appear to be quite well incorporated in FFA crystals.

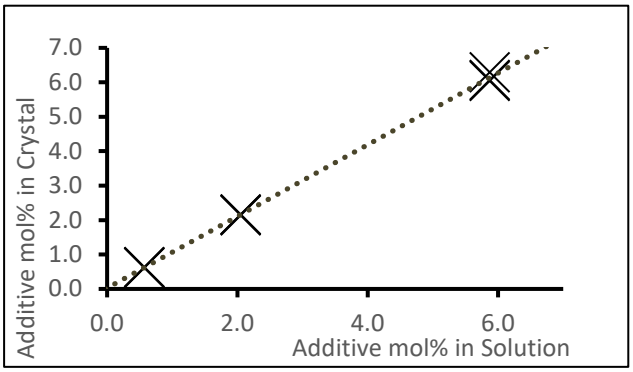

Fig. 3. Plot of additive incorporation *vs.* additive level for crystals of FFA grown from MeOH solutions containing 0 to 6 % MeFA.

Previous research had shown stepwise dissolution to be useful for analysing the distribution of impurities within crystals[13,14] hence that approach has been further developed in this work for application to FFA crystals. Samples of pure FFA crystals were used for the initial method development while samples of impure FFA crystals were subsequently studied. Pure FFA crystals were measured by image analysis software to determine the length and surface area of each crystal. The mass of the sample was also measured. Hexane was selected as the dissolution medium due to the moderate solubility of FFA in that solvent (2.40 mg ml^{-1} at 25 °C). Figure 4 shows the surface areas, determined by image analysis, of a sample of 49 FFA crystals over four stepwise dissolution stages, allowing the effect of the partial dissolution steps on the overall sample of crystals to be tracked, showing that an approximately similar degree of dissolution can be obtained on all the particles in the sample and that the sample can be partially dissolved in stages. Images of FFA crystals, containing MeFA and *t*BuFA impurities, after a series of partial dissolution stages are shown in the ESI, Figures S29 and S30, showing that the edges of crystals recede at similar rates. This dissolution approach is applicable provided the particles, whether single crystals or polycrystalline, are capable of existing as kinetically independent particles after each dissolution step, with or without stabilisation by surfactants. The approach has been shown to be applicable to FFA crystals of under 100 μm size.

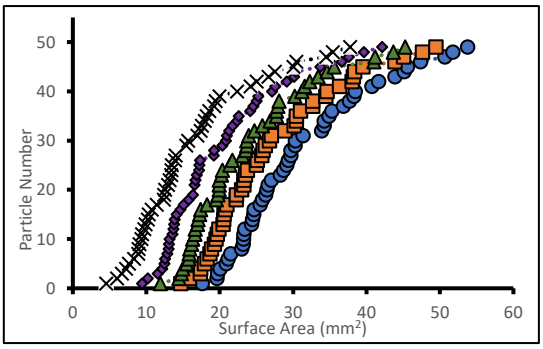

Fig. 4. Surface area distribution plots of a sample of FFA crystals over four dissolution stages, (•) showing the size (by surface area) distribution before any dissolution stages (pre-dissolution), (□) the distribution after the 1st partial dissolution (PD1), (Δ) after PD2, (◊) after PD3, (x) after PD4.

Figure 5 presents levels of MeFA impurity measured in solutions obtained by partial dissolution of FFA crystals. Data for FFA crystals grown from solutions containing 0.5% MeFA impurity and from solutions containing 5.0% MeFA impurity are shown. The dissolution stage is characterised by the percent of dissolution corresponding to the 'dissolution mid-point', i.e., quantifying the extent of dissolution where 0% represents no dissolution and 100% complete dissolution, the mid-point of the difference between mass values for the sample of crystals before and after the dissolution step. An increasing trend is observed across successive dissolution stages in both sets of data implying that a slightly higher level of impurity is incorporated at the start of crystallisation, and a progressively lower amount as the crystals grow larger.

Studies on the crystallization of proteins and related macromolecules have characterized certain impurities in terms of incorporation at earlier or later stages of crystal growth. Micro-heterogeneous impurities, which differ in certain aspects to the crystallising substance but retain an overall similarity, tend to be preferentially incorporated at the early stages of crystal nucleation and growth.[29,30] It is reasonable that MeFA, which has a relatively modest difference in structure relative to FAA, can be seen to exhibit this pattern of behaviour.

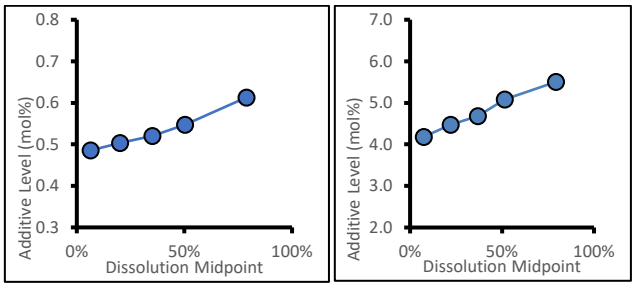

Fig. 5. Plots of MeFA impurity level *vs.* dissolution midpoint of samples of FFA crystals grown with **(left)** approx. 0.5 % MeFA impurity and **(right)** with approx. 5 % MeFA impurity.

The crystals studied by the partial dissolution analyses described above had relatively prismatic morphologies. However, FFA crystals, in common with many pharmaceutical and organic compounds, often display fine or needle-like morphologies. The partial dissolution approach can be usefully applied to crystals with such morphologies (Figure 6). It was found that crystals containing ca. 0.5 % MeFA can form fine tabular crystals (ESI Figure S24). Samples

displaying this morphology were subjected to the partial dissolution process and the level of MeFA incorporation was found to vary between 0.56 % and 0.62 %. Crystals of FFA containing MeFA impurity also often grew as acicular crystals. The impurity levels for samples of FFA crystals with that morphology, when subjected to the partial dissolution approach, exhibits a slight increase across successive dissolution stages, suggesting a decrease in additive incorporation with crystal growth.

Crystals of FFA containing *t*BuFA impurity often gave smaller acicular needles, however the partial dissolution approach could still be applied (Figure 7). These crystals were found to share a similar pattern of additive incorporation, higher close to the surface of the crystals and less towards the centre. In studies on the crystallization of proteins, impurities which differ significantly in structure to that of the crystallising entities are referred to as heterogenous impurities and tend to be preferentially incorporated at the later stages of crystal growth.[29,30] It is reasonable that the behaviour of *t*BuFA is consistent with that, as the replacement of the trifluoromethyl group of FFA by the *tertiary*-butyl group of *t*BuFA constitutes a significant change in steric and electronic properties.

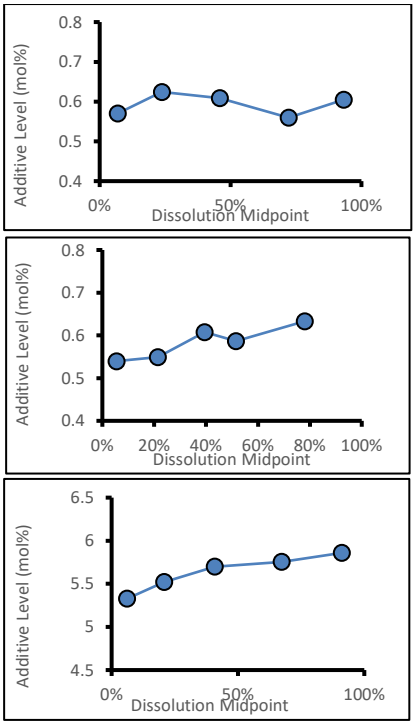

Fig. 6. (top) Plot of additive level *vs.* dissolution midpoint for fine tabular FFA crystals containing ca. 0.5% MeFA impurity.**–(centre)** Plot of additive level *vs.* dissolution midpoint of acicular FFA crystals containing ca. 0.5% MeFA impurity. **(bottom)** Plot of additive level *vs.* dissolution midpoint of acicular FFA crystals containing ca. 5 % MeFA impurity.

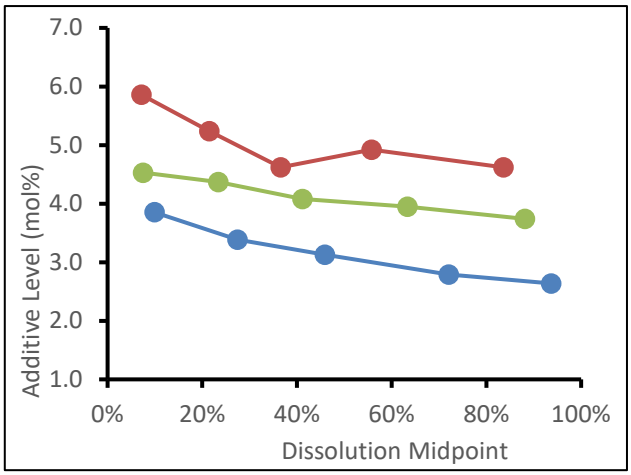

Fig. 7. Plots of additive level *vs.* dissolution midpoint of fine acicular FFA crystals containing ca. 3% (bottom), 4% (middle) or 5% (top) *t*BuFA impurity.

Long fine needle morphologies are relatively common for crystals of organic and pharmaceutical compounds, depending on the growth conditions. For FFA, slow cooling of saturated solutions from acetonitrile formed clusters with each long needle in the cluster growing outward from a single nucleation point. For crystals which are very long fine needles, the partial dissolution approach is no longer feasible. Extreme needles are not suitable for sizing by the methods used and achieving a relatively even level of partial dissolution is not feasible. An alternative approach for these crystals is to utilise the growth from a single nucleation point, which allows for the determination of the direction and extent of growth for each crystal. Samples of such crystals, containing between 2 and 6 % MeFA impurity, could be divided lengthwise into three segments, corresponding to different stages of crystal growth (Figure 8). The impurity levels in each of these segments were determined (Table 1) indicating a moderate increase in the extent of incorporation during the stages of crystal growth. The segmentation analysis approach is a feasible method of mapping impurity distributions in crystals with extremely needle-like morphologies but is not feasible for larger multi-crystal samples, although such extreme needle-like morphologies would normally be avoided in a process scale crystallisation.

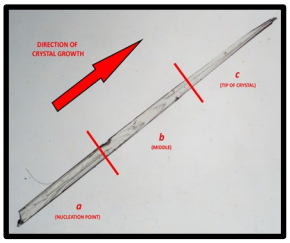

Fig. 8. Diagram of segmentation process on an acicular crystal of FFA, illustrating the direction of crystal growth and labelling of segments *a*, *b*, and *c*.

Table 1. Percentage MeFA impurity in segments *a*, *b* and *c*, as per Figure15, of FFA crystals occurring as very fine needles.

% MeFA in growth solns	% MeFA in crystal segments		
	a	*b*	*c*
2.01	2.09	2.16	2.25
3.12	3.17	3.14	3.38

Conclusions

The mode of incorporation of impurities in crystalline materials affects the purification performance of crystallisations.[3-7] HPLC is probably still the most widely used analytical method in process development and support and, as HPLC requires dissolution of the sample, the potential for achieving location-specific analysis through controlled dissolution exists.[31] This concept was demonstrated by previous work.[13,14] Extension to drug substance material displaying typical challenges such as polymorphism and non-prismatic morphologies is demonstrated in the current work on flufenamic acid (FFA) and two impurities, MeFA and *t*BuFA.

MeFA and *t*BuFA were obtained by modification of a literature[19] route. Evaluation of the phase of the FFA / impurity mixtures was complicated by the polymorphism of FFA. In line with work reported for FFA / mefenamic acid mixtures,[20] DSC data in this work was consistent for formation of an FFA Form III / MeFA solid solution with a thermal minimum.

Initially demonstration on samples of pure FFA crystals showed that crystals could be partially dissolved leaving an undissolved remainder. Application of this method allowed evaluation of the variation in MeFA and *t*BuFA impurity levels in FFA crystals, with impurity levels are shown as mol% varying with dissolution midpoint. This allows mapping of the variation of impurity level at locations of the crystals varying from the outer surface to the interior core. For the MeFA impurity, a gradual increase is most usually observed, corresponding to a gradual decrease in incorporation during crystal growth. For the *t*BuFA impurity, an opposite effect was observed. The *t*BuFA impurity was selected as an impurity as the behaviour was likely to be less predictable than that of the simple CF_3 to CH_3 replacement of MeFA and the finding to the stepwise dissolution analysis in this case is consistent with that. Stepwise dissolution could usefully be applied to FFA crystals of various morphologies, including quite acicular crystals. However, for crystals with an extremely needle-like morphology, segmentation analysis was more practical. Analysis of segments of crystals give similar data on the variation of impurity level throughout the crystals but is less applicable to larger numbers of crystals than the stepwise dissolution approach.

Impurity management is a key part of process development particularly utilising crystallisation. The mode of impurity incorporation into the crystalline material obtained and the variation in impurity level, both between crystal particles and within particles, would be valuable data for optimising such processes. This requires analysis with can be specific to definable locations in crystal batches. Improved washing or slurrying would be worth examining in cases in which impurities are found to be largely on or near particle surfaces, while for cases in which impurities are present throughout particles, examination of crystallisation parameters would be indicated. In cases where impurities are more incorporated at the earlier or later stages of growth, appropriate consideration of nucleation strategy and control of cooling would be indicated.

A number of advanced and emerging technologies are likely to be of value for this aim. It would be useful to be able to utilise HPLC, as it is perhaps the most commonly used analytical method for process support and development. As HPLC requires dissolution, the dissolution process can also be used to control the region of sampling for analysis. With samples consisting of individual crystals, the dissolved regions can be directly related to crystal growth. That would not be the case with agglomerated particles, but dissolution, in conjunction with suitable particle sizing, would still give information on the level and uniformity of impurities.

The partial dissolution data shows that the MeFA and tBuFA impurities are present throughout the crystal particles, in similar levels depending on the amount of impurity in the crystallising medium, with moderate variations during crystal growth dependent on the crystallisation method. If such data were obtained for batches of FFA obtained by a process crystallisation, it would tend to direct the process team away from, for example, improved washing or slurrying to improve purity, and toward changing the crystallisation parameters, e.g. mode of nucleation and/or cooling rate, to improve impurity rejection during growth. The team might also examine any pre-crystallisation process chemistry to reduce the amount of the impurity in the crystallising medium. The work described above demonstrates the feasibility of this for an important pharmaceutical material, flufenamic acid, with regard to two related substances, MeFA and *t*BuFA, as impurities, but could be extended to the determination of other impurities and to other API/impurity systems, provided suitable HPLC methods are available. The approach could be utilised for a wide range of crystal habits, requiring modification only for extreme needle morphologies. Hence, widely available analytical and particle sizing techniques can be used to provide data on impurity levels which can be assigned to definable regions of molecular crystal batches.

Author Contributions

T.B., conceptualisation, investigation, writing; R. A. C., conceptualisation, funding acquisition, supervision, writing; H. A. M., conceptualisation, funding acquisition, supervision, writing.

Conflicts of interest

There are no conflicts to declare.

Acknowledgements

We are grateful to Alkermes Pharma Ire Ltd and the Irish Research Council for provision of support under grant number

EPSPG/2016/179 and to Science Foundation Ireland under grant number SFI 12/RC/2275_P2.

Notes and references

1. J. W. Mullin, Crystallization, 4th Edition, Butterworth-Heinemann, Oxford, 2001.
2. H. A. Moynihan and D. E. Horgan, *Org. Proc. Res. Dev.*, 2017, **21**, 689-704.
3. S. J. Unwin, G. Levilain, I. Marziano, J. M. Merritt, I. Houson and J. H. Ter Horst, *Org. Proc. Res. Dev.,* 2020, **24**, 1443-1456.
4. C. Darmali, S. Mansouri, N. Yazdanpanah and M. W. Woo, *Ind. Eng. Chem. Res.* 2019, **58**, 1463−1479.
5. H. Lorenz and W. Beckmann, *Cryst. Basic Concepts Ind. Appl.* 2013, 129−148.
6. S. J. Urwin, S. Yerdelen, I. Houson and J. H. ter Horst, *Crystals*, 2021, **11**, 1344.
7. Y. S. Cheng, K. W. Lam, K. M. Ng and C. Wibowo, *AIChE*, *J*. 2009, **56**, 633−649.
8. C. G. Moyers, *Chem. Eng. Prog.,* 1986, **82**, 42–46.
9. J. A. Hayes, K. S. Eccles, S. E. Lawrence and H. A. Moynihan, *Carbohyd. Res.,* 2016, **425**, 35-39.
10. S. Ottoboni, M. Chrubasik, L. Mir Bruce, T. Thu Hien Nguyen, M. Robertson, B. Johnston, I. D. H. Oswald, A. Florence and C. Proce, *Cryst. Growth Des.,* 2018, **18**, 2750-2758.
11. Y. Xiao, Z. Pan, P. Duan, J. Yuan, B. Kong, *CrystEngComm*, 2024, **26**, 3455-3458.
12. A. Adawy, W. J. P. van Enckevort, E. S. Pierson, W. J. de Grip, E. Vlieg, *CrystEngComm*, 2014, **16**, 9800-9809.
13. H. A. Moynihan and D. Armstrong, *CrystEngComm*, 2018, **20**, 2617–2633.
14. H. A. Moynihan and D. Armstrong, *RSC Advances*, 2019, **9**, 21405-21417.
15. P. Prasher and M. Sharma, *Drug Dev. Res.* 2021**, 82**, 945-958.
16. V. López-Mejías, J. W. Kampf and A. J. Matzger, *J. Am. Chem. Soc.,* 2012, **134**, 9872-9875.
17. K. Zhang, N. Fellah, V. López-Mejías and M. D. Ward, *Cryst. Growth Des.,* 2020, **20**, 7098-7103.
18. X. He, J. G. Stowell, K. R. Morris, R. R. Pfeiffer, H. Lui, P. Stahly and S. R. Byrn, *Cryst. Growth Des.,* 2001, **1**, 305-312.
19. R. F. Pellón, R. Carrasco, T. Márquez and T. Mamposo, *Tetrahedron Lett.* 1997, **38**, 5107–5110.
20. E. H. Lee and S. R. Byrn, *J. Pharm. Sci.* 2010, **99**, 4013–4022.
21. J. F. McConnell, *Cryst. Struct. Commun.,* 1973, **3**, 459–461.
22. H. M. Krishna Murthy, T. N. Bhat and M. Vijayan, *Acta Cryst. B – Structural Science*, 1982, **38**, 315–317.
23. J. Krc, *Microscope* 1977, **25**, 31–45.
24. J. Potticary, C. L. Hall, R. Guo, S. L. Price, S. R. Hall, *Cryst. Growth Des.*, 2021, **21**, 6254-6265.
25. E. H. Lee, S. M. X. Boerrigter, S. R. Byrn, *Cryst. Growth Des.*, 2010, **10**, 518-527.
26. ImageJ https://imagej.nih.gov/ij.
27. C. A. Schneider, W. S. Rasband and K. W. Eliceiri, *Nat. Methods* 2012, **9**, 671–675.
28. S. P. Delaney, T. M. Smith, T. M. Korter, *J. Mol. Struct.* 2014, **1078**, 83–89.
29. A. Adawy, *Cryst. Growth Des.,* 2024, **24**, 6865-6887.
30. B. R. Thomas, A. A. Chernov, *J. Cryst. Growth*, 2001, **232**, 237-243.
31. A. Adawy, E. G. G. van der Heijden, J. Hekelaar, W. J. P. van Enckevort, W. J. de Grip, E. Vlieg, *Cryst. Growth Des.,* 2015, **15**, 1150-1159.